

# NPPB modulates apoptosis, proliferation, migration and extracellular matrix synthesis of conjunctival fibroblasts by inhibiting PI3K/AKT signaling

LIXIA SUN<sup>1,2</sup>, YARU DONG<sup>1</sup>, JING ZHAO<sup>1</sup>, YUAN YIN<sup>1</sup>, BAINAN TONG<sup>1</sup>, YAJUAN ZHENG<sup>1</sup> and HUA XIN<sup>3</sup>

<sup>1</sup>Department of Ophthalmology, The Second Hospital of Jilin University, Jilin University, Changchun, Jilin 130041;

<sup>2</sup>Department of Ophthalmology, Yanbian University Affiliated Hospital, Yanbian University, Yanji, Jilin 133000;

<sup>3</sup>China-Japan Union Hospital, Jilin University, Changchun, Jilin 130033, P.R. China

Received April 14, 2016; Accepted November 30, 2017

DOI: 10.3892/ijmm.2017.3323

**Abstract.** When treating glaucoma, excessive scar tissue reactions reduce the postoperative survival rate of the filtering bleb. Accumulating evidence has demonstrated that the proliferation, migration and extracellular matrix (ECM) synthesis of fibroblasts are important molecular mechanisms underlying scar formation. Recent evidence has demonstrated that chloride channels play an important role in controlling cell proliferation, apoptosis, migration and the cell cycle process in several cell types, but the effects of chloride channels on conjunctival fibroblasts have not been studied. The aim of the present study was to investigate the effects of the chloride channel blocker 5-nitro-2-(3-phenylpropylamino) benzoic acid (NPPB) on cell proliferation, apoptosis, migration, cell cycle progression and ECM synthesis in human conjunctival fibroblasts (HConFs), and to further investigate the mechanism of resistance to scar formation following glaucoma filtration surgery. HConFs were exposed to NPPB or lubiprostone. Cell proliferation and viability was evaluated using the Cell Counting Kit-8. Cell migration was measured using Transwell migration and scratch-wound assays. Flow cytometry was used to study apoptosis and cell cycle progression. Quantitative polymerase chain reaction and western blot analyses were performed to determine mRNA and protein expression levels, respectively. Following NPPB treatment, HConFs exhibited reduced proliferation and migration, along with increased apoptosis. NPPB also inhibited cell cycle progression by arresting cells in the

G0/G1 phase and reducing collagen I and fibronectin expression, as well as the phosphorylation of phosphoinositide 3-kinase (PI3K) and protein kinase B (AKT). However, lubiprostone treatment exerted the opposite effects on HConFs. Therefore, NPPB treatment inhibited proliferation, migration, cell cycle progression and synthesis of the ECM, while promoting apoptosis in HConFs, by inhibiting the PI3K/AKT signaling pathway.

## Introduction

Glaucoma is the most common cause of irreversible blindness worldwide and severely affects the visual function and quality of life of the patients (1,2). Filtration surgery is the most common treatment for reducing intraocular pressure, but excessive scar tissue formation in the filtration area reduces the postoperative 5-year survival rate of the filtering bleb to <50% (3,4). Several anti-scarring regimens, such as mitomycin C (MMC) or 5-fluorouracil (5-FU), are currently used to improve the results of glaucoma surgery, but are of limited use clinically due to severe complications, such as filtering bleb leakage, corneal epithelial dysfunction, late-onset endophthalmitis and macular degeneration (5-8). Therefore, safer and more effective anti-scarring agents are urgently required.

Human conjunctival fibroblasts (HConFs) are located in subconjunctival connective tissue, which plays an important role in scar tissue reactions of the filtering bleb. Filtration surgery may stimulate conjunctival fibroblast proliferation, migration, differentiation from fibroblasts to myofibroblasts, and promote the secretion of extracellular matrix (ECM); these are important processes of wound healing, but may also lead to scarring (9-11). The role of ion channels (chloride channels in particular) in the development of fibrosis have attracted increasing attention in recent years (12-15). Previous findings have demonstrated that chloride channels are widely distributed in mammalian tissues and organs and various types of cells, and play important roles in regulating cell cycle progression, cell proliferation, migration and apoptosis by maintaining the cell volume balance (16-24). The phosphatidylinositol 3-kinase (PI3K)/protein kinase B (AKT) signaling pathway is a survival pathway that has recently become known as a key regulator of cell proliferation, migration and apoptosis (25,26).

*Correspondence to:* Dr Yajuan Zheng, Department of Ophthalmology, The Second Hospital of Jilin University, Jilin University, 218 Ziqiang Road, Nanguan, Changchun, Jilin 130041, P.R. China

E-mail: zhengyajuan124@126.com

Professor Hua Xin, China-Japan Union Hospital, Jilin University, 126 Xiantai Street, Changchun, Jilin 130033, P.R. China

E-mail: 13596118509@163.com

**Key words:** collagen I, fibronectin, 5-nitro-2-(3-phenylpropylamino) benzoic acid, conjunctival fibroblasts, cell proliferation, apoptosis, cell migration, phosphoinositide 3-kinase/protein kinase B

The PI3K/AKT pathway also plays a key role in regulating ECM synthesis (27). We previously cloned the ClC-2 gene, which was sensitive to changing cell volumes, and revealed its important roles in the processes of cell differentiation, proliferation and division (17,18). The chloride channel blocker 5-nitro-2-(3-phenylpropylamino) benzoic acid (NPPB) is known to selectively block volume-sensitive, hyperpolarization-activated and medium-conductance Cl channels. NPPB is not highly selective, but is used by numerous investigators to examine the pharmacological properties of Cl ion currents in various cells. Cheng *et al.* (19) observed that NPPB increased apoptosis in human bronchial epithelial cells. We previously found that the chloride channel blocker NPPB inhibited the transition of quiescent (G0) fibroblasts into the cell cycle (17). However, it remains unclear whether or how NPPB affects the proliferation, migration and ECM synthesis of conjunctival fibroblasts.

In the present study, HConFs were cultured to investigate the effects of the chloride channel blocker NPPB on the proliferation, migration, apoptosis and ECM synthesis of HConFs. It was further investigated whether NPPB exerts the above-mentioned effects on HConFs via the PI3K/AKT signaling pathway to provide novel insights into prevention of glaucoma filtration surgery scar formation.

## Materials and methods

**Drugs.** NPPB and lubiprostone (both from Sigma-Aldrich; Merck KGaA, St. Louis, MO, USA) were prepared as 0.4 and 0.1 M stock solutions in dimethyl sulfoxide (DMSO) (Beyotime Institute of Biotechnology, Jiangsu, China), respectively, stored at a temperature  $< -20^{\circ}\text{C}$ , and protected from light until use. NPPB and lubiprostone were diluted to 10–200  $\mu\text{M}$  and 10–300 nM, respectively, in Dulbecco's modified Eagle's medium (DMEM) (Sigma-Aldrich; Merck KGaA) containing 10% fetal bovine serum (FBS) (Invitrogen/Gibco; Thermo Fisher Scientific, Grand Island, NY, USA) on the day of the experiment. The highest concentration of DMSO in the test solutions was 0.1%. To exclude the possibility that proliferation was inhibited by DMSO, cells were exposed to a final DMSO concentration of 0.1% in DMEM containing 10% FBS.

**Cell lines and cell culture.** HConFs from ScienCell Research Laboratories (San Diego, CA, USA) were isolated from the human conjunctiva. HConFs are characterized by a spindle-shaped morphology and positivity for immunofluorescence staining with anti-fibronectin antibodies. HConFs were maintained and cultured at  $37^{\circ}\text{C}$  in a humidified incubator with 5%  $\text{CO}_2$  in fibroblast medium (ScienCell Research Laboratories) containing fibroblast growth supplement (undisclosed formulation), 2% FBS, 100 U/ml penicillin and 100  $\mu\text{g}/\text{ml}$  streptomycin.

**Cell proliferation assay [Cell Counting Kit-8 (CCK-8) assay].** HConF suspensions were transferred to a 96-well plates (200  $\mu\text{l}/\text{well}$ ) with a density of  $0.5 \times 10^4$  cells/well for 24 h. The cells were then treated with media containing different reagents for 48 h. Subsequently, each well was incubated with 10  $\mu\text{l}$  CCK-8 solution (BestBio, Jiangsu, China) for a further 3 h at  $37^{\circ}\text{C}$ . The absorbance, expressed as optical density (OD), was recorded at 450 nm using an automated microplate reader (model 3001-1387; Thermo Fisher Scientific, Inc., Waltham, MA, USA).

**Cell apoptosis assay.** Annexin V binding to HConF was performed using an Annexin V-FITC Apoptosis kit (BestBio) to measure apoptosis. HConFs ( $5 \times 10^5/\text{well}$ ) were plated into 6-well plates and then treated with medium containing different reagents for 48 h. Briefly, the cells, after being rinsed twice with phosphate-buffered saline (PBS), were resuspended in 400  $\mu\text{l}$  of 1X binding buffer (10 mM HEPES, 140 mM NaCl, 2.5 mM  $\text{CaCl}_2$ ; pH 7.4), to which 5  $\mu\text{l}$  of Annexin V-FITC was added and mixed well. After a 15-min incubation period at  $2-8^{\circ}\text{C}$  in the dark, 10  $\mu\text{l}$  of propidium iodide (PI) was added to the cells and mixed well. The cells were incubated for a further 5 min at  $2-8^{\circ}\text{C}$  in the dark, after which time flow cytometry (Cytomics FV 500; Beckman Coulter, Brea, CA, USA) was performed within 15 min.

**Cell cycle analysis.** The cell cycle status was assessed by flow cytometry using a Cell Cycle and Apoptosis Analysis kit (Beyotime Institute of Biotechnology). Briefly, the cells were grown in 100-mm plates with 10% FBS for 24 h. After treating the cells with media containing different reagents for 48 h, they were collected and fixed in 75% ethanol for 24 h at  $4^{\circ}\text{C}$ . After rinsing the cells with PBS, they were stained with PI buffer (containing 500  $\mu\text{l}$  staining buffer, 25  $\mu\text{l}$  of 20X PI and 10  $\mu\text{l}$  of 50X RNase). The cell cycle distribution was assessed by flow cytometry (Cytomics FV 500; Beckman Coulter).

**Scratch-wound assay.** HConFs ( $5 \times 10^5$  cells/well) were plated into 6-well plates in culture medium. At 24 h after seeding, the culture medium was replaced with fresh medium supplemented with 4  $\mu\text{g}/\text{ml}$  MMC (Zhejiang Hisun Pharmaceutical Co., Ltd., Taizhou, China). After a 2-h incubation, a line was scratched into confluent cell monolayers using a sterile 200- $\mu\text{l}$  pipette tip, and the cells were washed 3 times with PBS. The scratch wound was allowed to heal for 12 h in the presence of different reagents. Micrographs were captured for each sample at 0 and 12 h, and the migration capacity of HConFs was evaluated by measuring the width of the scratch wound at both time-points, using ImageJ software, version 1.5 (produced by Java2HTML).

**Transwell migration assay.** The chemomigration assay was performed in Transwell plates (pore size, 8  $\mu\text{m}$ ; Corning Costar, Inc., Corning, NY, USA). The chambers were inserted into a 24-well plate. Cells ( $1 \times 10^5$ ) were suspended in 200  $\mu\text{l}$  DMEM and added to the upper chamber. Our preliminary experiments demonstrated that an FBS concentration of 10% is optimal for observing cell migration (data not shown). Therefore, DMEM with 10% FBS was added into the lower chamber of each well, and the cells were incubated for 12 h. The medium and non-migrated cells in the upper chamber were removed gently with a cotton swab, whereas the migrated cells in the lower chamber were fixed with paraformaldehyde (4%) and stained with crystal violet. Images were captured at a magnification of  $\times 200$ . Cells in 6 different fields were counted.

**Western blot analysis.** Cells were washed with pre-cooled PBS and lysed in radioimmunoprecipitation assay buffer containing the protease inhibitor phenylmethylsulfonyl fluoride and the phosphatase inhibitor  $\text{Na}_3\text{VO}_4$  (Nanjing KeyGen Biotech Co., Ltd., Nanjing, China) on ice. Subsequently, the cells were gently scraped with a rubber policeman and centrifuged

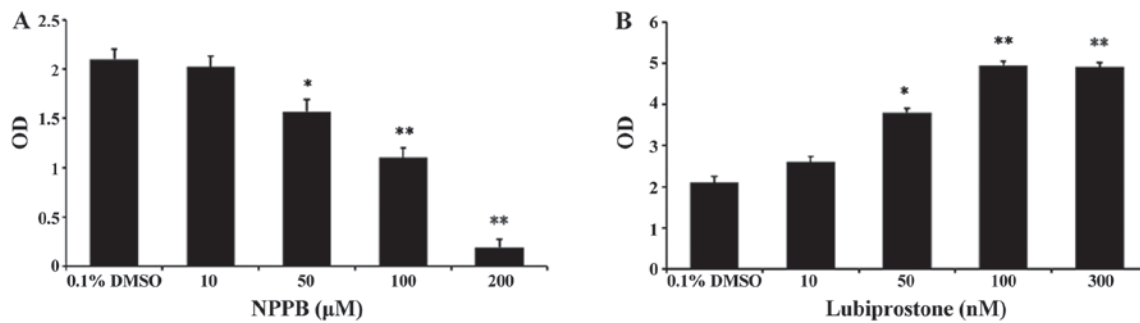


Figure 1. Effects of the chloride channel blocker 5-nitro-2-(3-phenylpropylamino) benzoic acid (NPPB) and the chloride channel activator lubiprostone on human conjunctival fibroblasts (HConF) proliferation. Relative cell numbers were detected using the Cell Counting Kit-8 assay and expressed as the optical density (OD) value. (A) Concentration-dependent inhibition of different concentration of NPPB (10-200  $\mu$ M) on cell proliferation after a 48-h stimulation. (B) Stimulation with <100 nM lubiprostone promoted cell proliferation in dose-dependent manner, but cell proliferation was no further promoted when the concentration of lubiprostone exceeded 100 nM (\* $P$ <0.05, \*\* $P$ <0.01 vs. control). DMSO, dimethyl sulfoxide.

at 1,500  $\times$  g for 12 min at 4°C. Protein concentrations were measured using the bicinchoninic acid (BCA) method with the enhanced BCA protein assay kit (cat. no. P0009; Beyotime institute of Biotechnology).

A total of 20  $\mu$ g of protein per sample was separated by 6-15% sodium dodecyl sulfate-polyacrylamide gel electrophoresis and transferred onto polyvinylidene fluoride membranes. The membranes were then blocked with 5% non-fat dry milk in Tris-buffered saline with 0.1% Tween-20 (TBST) for 1 h at 37°C and incubated overnight at 4°C in TBST with mouse monoclonal anti-collagen I (1:2,500 dilution, cat. no. ab88147) and rabbit polyclonal anti-fibronectin (1:1,500 dilution, cat. no. ab2375) (both from Abcam, Cambridge, UK), mouse monoclonal anti-PI3 kinase p85 (1:500 dilution, cat. no. sc-1637), mouse polyclonal anti-p-PI 3-kinase p85 $\alpha$  (1:500 dilution, cat. no. sc-12929), mouse monoclonal anti-Akt1 (1:500 dilution, cat. no. sc-5298), mouse monoclonal anti-p-Akt1 (1:500 dilution, cat. no. sc-293125) (all from Santa Cruz Biotechnology, Inc., Santa Cruz, CA, USA), and/or mouse monoclonal anti- $\beta$ -actin (1:1,000 dilution, cat. no. AF0003; Beyotime Institute of Biotechnology) antibodies. Following two washes with TBST, the membrane was incubated with horseradish peroxidase-conjugated goat anti-rabbit IgG secondary antibody (1:5,000 dilution, cat. no. A0208) or goat anti-mouse IgG secondary antibody (1:5,000 dilution, cat. no. A0129) (both from Beyotime Institute of Biotechnology) for another 1 h at room temperature and washed 3 times with TBST. Detection was performed with enhanced chemiluminescence western blotting reagents (Beyotime Institute of Biotechnology) and the membranes were visualized by exposure to Kodak X-ray film. The results were scanned and analyzed using ImageJ software (National Institutes of Health, Bethesda, MD, USA).

**Reverse transcription-quantitative polymerase chain reaction (RT-qPCR).** Total RNA was extracted from HConFs using the RNAiso Plus reagent (Takara Bio, Inc., Shiga, Japan), according to the manufacturer's instructions. Single-stranded cDNA templates were prepared from 500 ng total RNA using the RT-for-PCR kit (Takara Bio, Inc.), according to the manufacturer's instructions. Specific cDNAs were subsequently amplified by PCR using the following primers (Shanghai R&S Biotechnology Co., Ltd., Shanghai, China): Collagen I forward, 5'-TCCTCTTAGCACCCCTTTCG-3' and reverse, 5'-GGACCA

GCAACACCATCTG-3'; fibronectin forward, 5'-CCAGCAGAG GCATAAGGTTTC-3' and reverse, 5'-CACTCATCTCCAACG GCATA-3'; GAPDH forward, 5'-CAGGAGGCATTGCTGATG AT-3' and reverse, 5'-CAGGAGGCATTGCTGATGAT-3'. PCR amplification from cDNA was performed using a LightCycler® 480 system (Roche Diagnostics, Basel, Switzerland) in a final reaction volume of 20  $\mu$ l containing 2X SYBR-Green mix (10  $\mu$ l; Toyobo Co., Ltd., Osaka, Japan), 1  $\mu$ l primer mix, 1  $\mu$ l template DNA and 8  $\mu$ l diethylpyrocarbonate water. The following cycling conditions were used: Initial denaturation at 95°C for 30 sec; 40 cycles of denaturation at 95°C for 15 sec, annealing at 59°C for 20 sec, elongation at 72°C for 20 sec; and a final extension at 72°C for 10 min. The data were normalized to GAPDH mRNA expression, using the  $\Delta\Delta$ Cq method (22).

**Statistical analysis.** Data are expressed as the mean  $\pm$  standard error (number of observations) and were analyzed using the Student's t-test and one-way analysis of variance. Statistical significance was defined as  $P$ <0.05. All experiments were repeated 4 times.

## Results

**Effect of NPPB on cell proliferation.** To assess the effects of the chloride channel blocker NPPB and the chloride channel activator lubiprostone on HConF cell proliferation, HConFs were first stimulated with different concentrations of NPPB (10, 50, 100 and 200  $\mu$ M) for 48 h using 0.1% DMSO as control. NPPB inhibited HConF proliferation in a dose-dependent manner, and 100  $\mu$ M NPPB inhibited cell proliferation by  $47.62\pm 1.99\%$  ( $P$ <0.01 vs. control; Fig. 1A). Conversely, HConF stimulation with lubiprostone (10, 50, 100 and 300 nM) promoted cell proliferation in a dose-dependent manner, the effect of which peaked at 100 nM (Fig. 1B).

**Effect of NPPB on the cell cycle.** Next, HConFs were divided into 3 groups, which were exposed to 100  $\mu$ M NPPB (NPPB group), 100 nM lubiprostone (LUBI group) or 0.1% DMSO as control (0.1% DMSO group). The effects of these treatments on cell cycle progression were tested by flow cytometry. The proportion of cells in G0/G1 in the 0.1% DMSO, NPPB and LUBI groups was  $64.43\pm 4.21$ ,  $81.44\pm 3.15$  and  $39.40\pm 2.14\%$ , respectively. The proportion of cells in S phase in the 0.1% DMSO, NPPB and LUBI

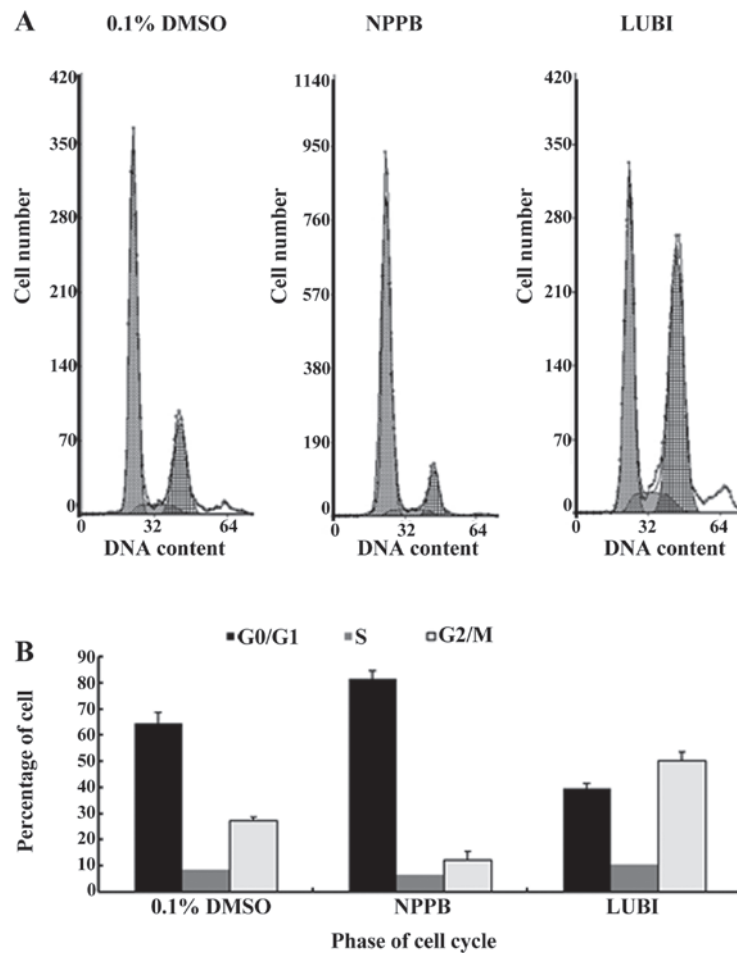


Figure 2. Effects of the chloride channel blocker 5-nitro-2-(3-phenylpropylamino) benzoic acid (NPPB) and the chloride channel activator lubiprostone (LUBI) on human conjunctival fibroblast (HConF) cell cycle progression, as determined by flow cytometry. (A) Typical cell cycle distribution of cells treated with 100  $\mu$ M NPPB or 100 nM lubiprostone for 48 h. (B) Quantitative distribution of cells in different phases after receiving different treatments (mean  $\pm$  standard error).

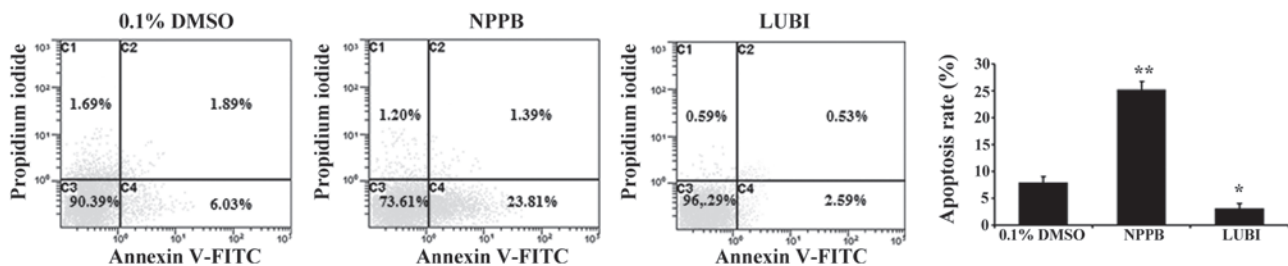


Figure 3. Human conjunctival fibroblasts (HConFs) were treated with 100  $\mu$ M 5-nitro-2-(3-phenylpropylamino) benzoic acid (NPPB) or 100 nM lubiprostone (LUBI) for 48 h, stained with Annexin V-FITC (x-axis) and propidium iodide (y-axis), and analyzed by flow cytometry. For each dot plot, the upper and lower right quadrants represent early and late apoptotic cells, respectively. Total apoptosis refers to the sum of early and late apoptosis values. Results are expressed as the mean  $\pm$  standard deviation from 4 independent experiments (\*\* $P$ <0.01, \* $P$ <0.05 vs. control).

groups was  $8.37 \pm 2.02$ ,  $6.56 \pm 2.21$  and  $10.30 \pm 3.09\%$ , respectively. The proportion of cells in G2/M phase in the 0.1% DMSO, NPPB and LUBI groups was  $27.20 \pm 1.32$ ,  $12.00 \pm 3.56$  and  $50.30 \pm 3.23\%$ , respectively. Therefore, NPPB inhibited cell cycle progression by arresting the cells in the G0/G1 phase, but lubiprostone promoted cell cycle progression by advancing the cells from G0/G1 to the S and G2/M phase (Fig. 2).

**Effect of NPPB on cell apoptosis.** To investigate the effect of NPPB on HConF apoptosis, HConFs were stimulated with

100  $\mu$ M NPPB or 100 nM lubiprostone for 48 h, using 0.1% DMSO as control. Treatment with 100  $\mu$ M NPPB for 48 h significantly increased the number of apoptotic HConFs compared with control treatment ( $25.2 \pm 1.5$  vs.  $7.92 \pm 1.1\%$ ;  $P$ <0.01). Treatment of HConFs with 100 nM lubiprostone resulted in a lower rate of apoptosis ( $3.12 \pm 0.88\%$ ;  $P$ <0.05 vs. control; Fig. 3).

**Effect of NPPB on cell migration.** The migration capacity of HConFs was measured via *in vitro* scratch and Transwell migration assays. The scratch-wound assay revealed

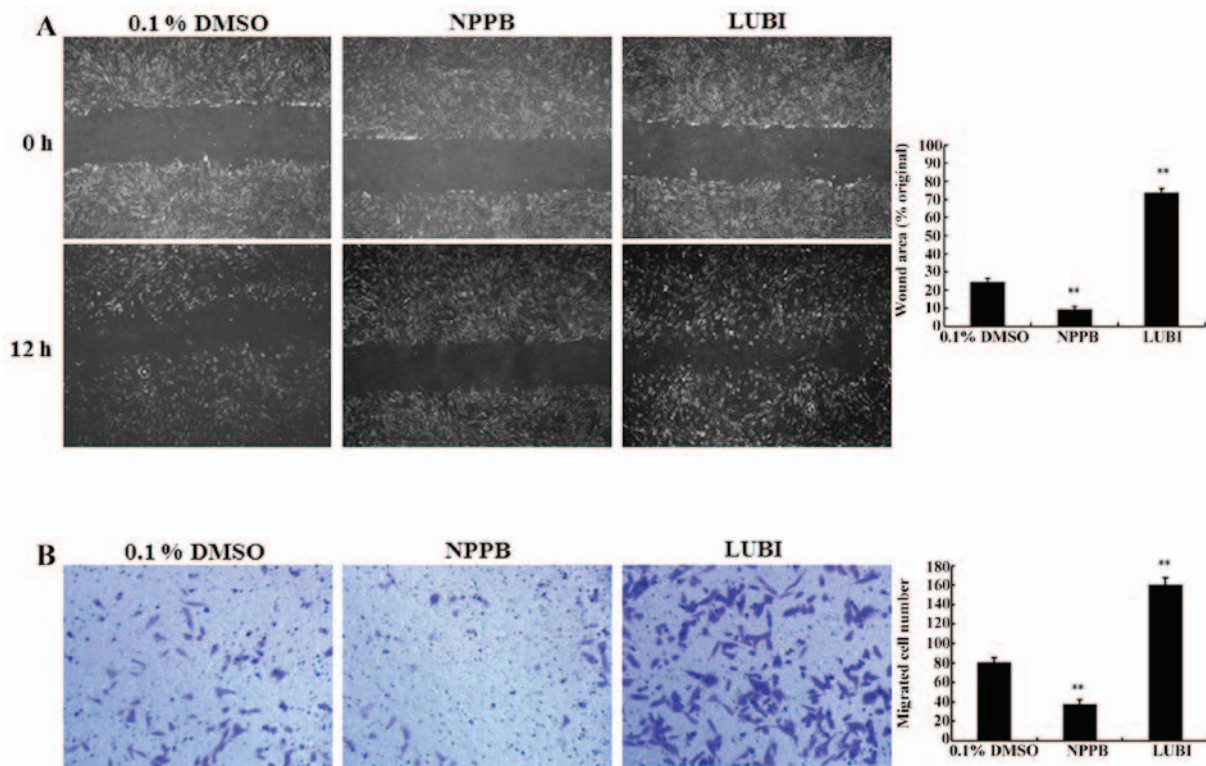


Figure 4. Effects of the chloride channel blocker 5-nitro-2-(3-phenylpropylamino) benzoic acid (NPPB) and the chloride channel activator lubiprostone (LUBI) on human conjunctival fibroblast (HConF) cell migration, assessed *in vitro* by performing scratch-wound and Transwell migration assays. The migratory ability of HConFs was determined by measuring the width of the scratch wound and the number of cells migrating to the lower chamber after 12 h. (A) Representative images of the scratch-wound assay results and quantification of the inhibitory effects of NPPB on HConF migration. (B) Representative images of Transwell migration assay results and quantification of the inhibitory effects of NPPB on HConF migration (\*\* $P < 0.01$  vs. control). DMSO, dimethyl sulfoxide.

that treatment with NPPB significantly inhibited wound healing compared with that observed in the control group ( $9.36 \pm 1.44$  vs.  $24.54 \pm 1.82\%$ , respectively;  $P < 0.01$ ). Treatment of HConFs with 100 nM lubiprostone significantly increased wound healing compared to that observed in the control group ( $73.83 \pm 2.26$ ,  $P < 0.01$  vs. control; Fig. 4A).

To confirm the results of the scratch-wound assay, a Transwell-migration assay was performed. As shown in Fig. 4B, significantly fewer HConFs migrated through the Transwell membrane in the NPPB group compared with the control group ( $7.41 \pm 0.83$  vs.  $20.55 \pm 1.02$  cells, respectively;  $P < 0.01$ ). A significantly greater number of cells migrated through the Transwell membrane in the LUBI group compared with the control group ( $41.58 \pm 0.89$ ;  $P < 0.01$  vs. control). These results indicated that NPPB inhibited and that lubiprostone promoted HConF migration (Fig. 4B).

#### Effect of NPPB on collagen I and fibronectin expression.

To evaluate the effects of NPPB on ECM production, the mRNA and protein expression of collagen I and fibronectin in the three groups were measured. The relative quantification results revealed that HConFs treated with NPPB exhibited significantly inhibited collagen I and fibronectin expression, at both the mRNA and protein levels. By contrast, the mRNA and protein expression of collagen I and fibronectin significantly increased in the lubiprostone group (Fig. 5).

*NPPB repressed the PI3K/Akt pathways.* Western blot analysis revealed that NPPB treatment significantly decreased the levels of p-PI3K and p-AKT (both  $P < 0.05$  vs. control).

Lubiprostone significantly increased the expression of p-PI3K and p-Akt ( $P < 0.05$  vs. control; Fig. 6).

## Discussion

Excessive postoperative conjunctival scarring at filtering bleb sites is the main reason underlying trabeculectomy failure. In general, this process consists of a series of events, including conjunctival fibroblast migration and proliferation, deposition, and contraction of dense collagen fibers after the proliferation of fibroblasts, which leads to aqueous outflow blockage by creating adhesions between the conjunctiva and episclera, as well as between the scleral flap and underlying tissues (28,29). Accumulating evidence suggests that chloride channels are critical for cell proliferation and apoptosis (30-32). NPPB was found to inhibit cell proliferation in a concentration- and time-dependent manner in nasopharyngeal carcinoma cells (30). NPPB also reduced cell proliferation in a concentration-dependent manner in mouse mesenchymal stem cells (31). Consistent with previous data, we observed that NPPB inhibited HConF proliferation in a dose-dependent manner. Data from our previous study demonstrated that the chloride channel blocker NPPB inhibits the transition of quiescent (G0) fibroblasts synchronized by serum deprivation/replenishment reentry into the proliferating phase by impairing passage through G1/S (17). Tao *et al* (31) reported that inhibiting Cl<sup>-</sup> currents using NPPB retained mouse mesenchymal stem cells in the G0/G1 phase and decreased the distribution of cells in S phase. NPPB inhibited the volume-activated chloride

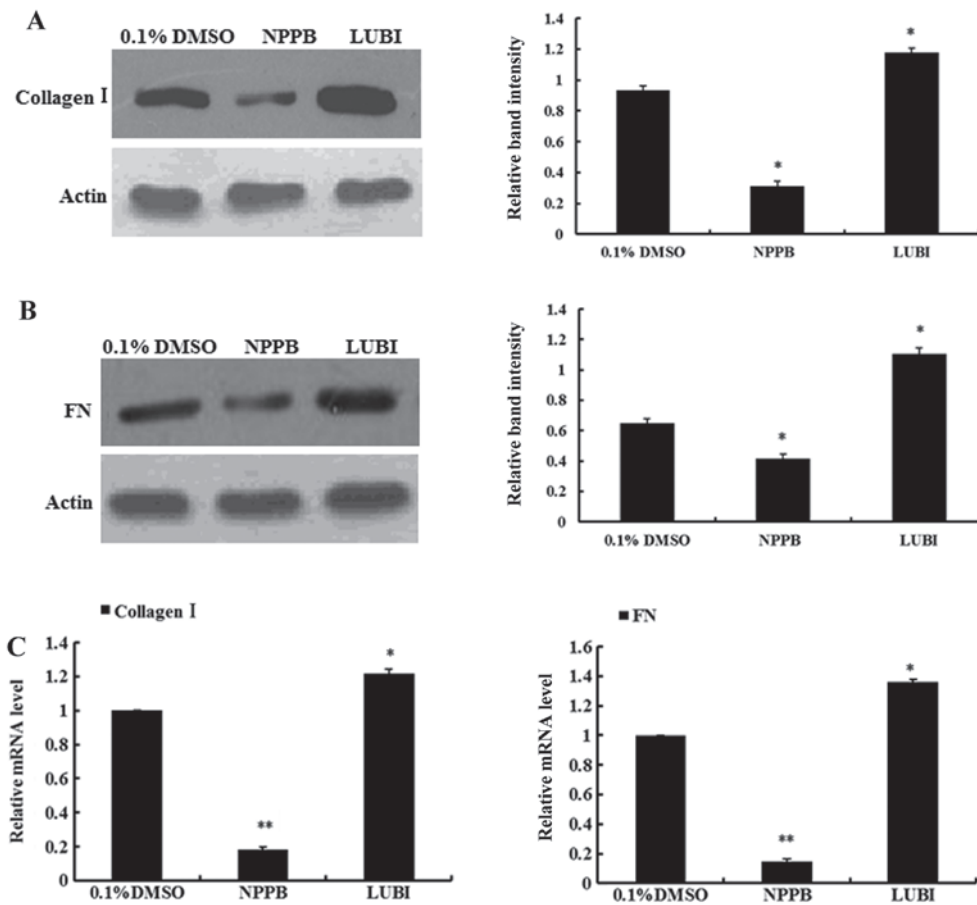


Figure 5. 5-Nitro-2-(3-phenylpropylamino) benzoic acid (NPPB) inhibits collagen I and fibronectin (FN) expression in human conjunctival fibroblasts (HConFs) at the mRNA and protein levels. HConFs were pretreated with NPPB (100  $\mu$ M), lubiprostone (LUBI; 100 nM), or 0.1% dimethyl sulfoxide (DMSO) as a vehicle control for 48 h. Quantitative polymerase chain reaction and western blot analyses were performed and the data shown represent the mean  $\pm$  standard deviation of 4 experiments. (A) Protein expression of collagen I in HConFs. (B) Protein expression of FN in HConFs. (C) mRNA expression of collagen I and FN in HConFs (\*\* $P$ <0.01, \* $P$ <0.05 vs. control).

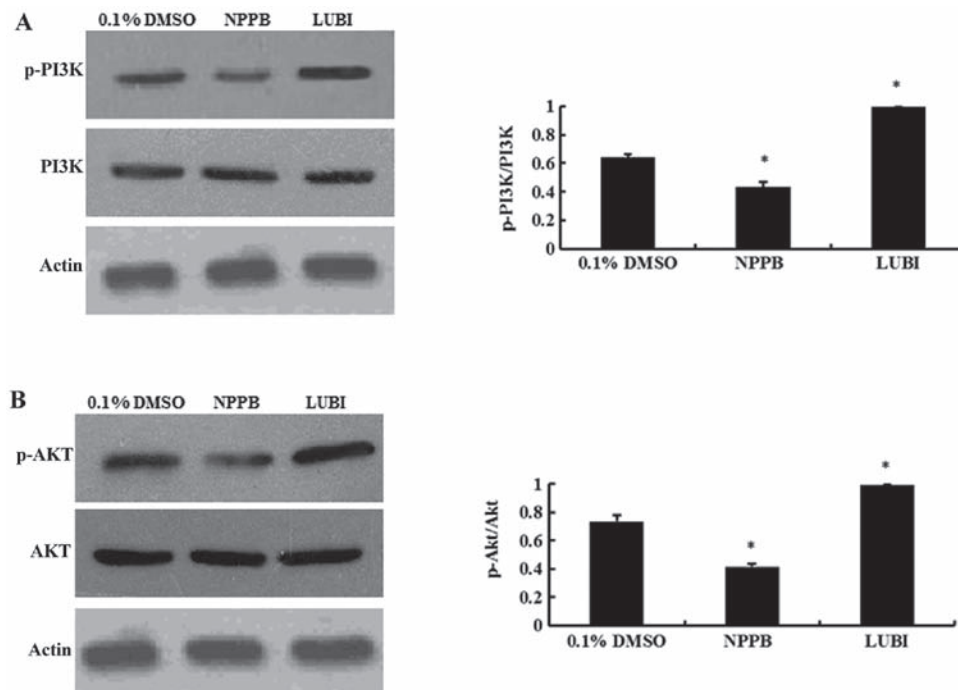


Figure 6. 5-Nitro-2-(3-phenylpropylamino) benzoic acid (NPPB) suppressed activation of the phosphoinositide 3-kinase (PI3K)/protein kinase B (AKT) signaling pathway. (A) Protein expression of phosphorylated PI3K in human conjunctival fibroblasts (HConFs). (B) Protein expression of phosphorylated AKT in HConFs ( $P$ <0.05 vs. control). DMSO, dimethyl sulfoxide; LUBI, lubiprostone.

current and proliferation of nasopharyngeal carcinoma cells in a dose-dependent manner, inhibited cell cycle progression and arrested cells at the G0/G1 phase boundary (32). To further investigate how NPPB participates in HConF proliferation, flow cytometry experiments were conducted and demonstrated that NPPB inhibited cell cycle progression and arrested cells at the G0/G1 phase boundary. Moreover, NPPB increased the abundance of the apoptotic HConF population, which was prevented by the chloride channel activator lubiprostone. In agreement with our findings, Souktani *et al* (33) found that NPPB increased apoptosis in rabbit myocardial cells. Cheng *et al* (19) reported that, both stimulation with NPPB and knocking down the expression of the CLC-3 chloride channel increased apoptosis; by contrast, overexpression of CLC-3 prevented TGF- $\beta$ 1-induced apoptosis in human bronchial epithelial cells. Contradictory data were also reported, indicating that NPPB inhibited apoptosis, instead of accelerating it (34,35). In CNE-2Z cells, NPPB prevented apoptosis induced by paclitaxel (36). The selectivity of NPPB for chloride channels in different cell types may account for the conflicting effects of NPPB on apoptosis.

The PI3K/AKT pathway is a survival pathway that regulates cell proliferation, apoptosis, differentiation and migration (37). The PI3K/AKT pathway may play key roles in the physiology and pathophysiology of several types of cells (38-41). The key enzyme of this pathway, PI3K, converts phosphatidylinositol 4,5-biphosphate to phosphatidylinositol 3,4,5-triphosphate, which binds both AKT and 3-phosphoinositide-dependent protein kinase 1 (PDK1), enabling PDK1 to phosphorylate AKT (41,42). The primary direct downstream target protein of PI3K is AKT. The activation of AKT causes a cascade of responses with downstream targets that regulate cellular functions. For example, AKT regulates cell migration via Rac1 and RhoA, increases cell survival via Bcl-2, and increases cell proliferation via the activation of the mammalian target of rapamycin (37,41). Zhou *et al* (26) reported that exendin-4 mediated proliferation, migration and apoptosis via the PI3K/AKT pathway in bone marrow mesenchymal stem cells. It has been reported that activation of PI3K/AKT signaling may induce the expression of ECM molecules in a number of cell types (43,44). Previous results demonstrated that inhibiting CIC-2 expression by RNA interference or a chloride channel blocker may attenuate cell proliferation and migration via the PI3K/AKT signaling pathway (45,46). Li *et al* (47) observed that suppression of PI3K/AKT signaling may decrease adhesion and migration of bone marrow-derived mesenchymal stem cells. In the present study, NPPB promoted cell apoptosis and inhibited proliferation, migration, cell cycle progression and synthesis of ECM, which paralleled suppressed expression of p-PI3K and p-AKT. Therefore, NPPB exerts the abovementioned effects on HConFs by inhibiting PI3K-dependent signaling.

## References

- Quigley HA and Broman AT: The number of people with glaucoma worldwide in 2010 and 2020. *Br J Ophthalmol* 90: 262-267, 2006.
- Foster PJ and Johnson GJ: Glaucoma in China: how big is the problem? *Br J Ophthalmol* 85: 1277-1282, 2001.
- Khaw PT, Chang L, Wong TT, Mead A, Daniels JT and Cordeiro MF: Modulation of wound healing after glaucoma surgery. *Curr Opin Ophthalmol* 12: 143-148, 2001.
- Lee DA: Antifibrosis agents and glaucoma surgery. *Invest Ophthalmol Vis Sci* 35: 3789-3791, 1994.
- Mielke C, Dawda VK and Anand N: Intraoperative 5-fluorouracil application during primary trabeculectomy in Nigeria: a comparative study. *Eye (Lond)* 17: 829-834, 2003.
- Wong TT, Khaw PT, Aung T, Foster PJ, Htoon HM, Oen FT, Gazzard G, Husain R, Devereux JG, Minassian D, *et al*: The Singapore 5-fluorouracil trabeculectomy study: effects on intraocular pressure control and disease progression at 3 years. *Ophthalmology* 116: 175-184, 2009.
- Shin DH, Ren J, Juzych MS, Hughes BA, Kim C, Song MS, Yang KJ and Glover KB: Primary glaucoma triple procedure in patients with primary open-angle glaucoma: the effect of mitomycin C in patients with and without prognostic factors for filtration failure. *Am J Ophthalmol* 125: 346-352, 1998.
- Perkins TW, Gangnon R, Ladd W, Kaufman PL and Heatley GA: Trabeculectomy with mitomycin C: intermediate-term results. *J Glaucoma* 7: 230-236, 1998.
- Chang L, Crowston JG, Cordeiro MF, Akbar AN and Khaw PT: The role of the immune system in conjunctival wound healing after glaucoma surgery. *Surv Ophthalmol* 45: 49-68, 2000.
- Atreides SP, Skuta GL and Reynolds AC: Wound healing modulation in glaucoma filtering surgery. *Int Ophthalmol Clin* 44: 61-106, 2004.
- Desjardins DC, Parrish RK II, Folberg R, Nevarez J, Heuer DK and Gressel MG: Wound healing after filtering surgery in owl monkeys. *Arch Ophthalmol* 104: 1835-1839, 1986.
- Song Y, Zhan L, Yu M, Huang C, Meng X, Ma T, Zhang L and Li J: TRPV4 channel inhibits TGF- $\beta$ 1-induced proliferation of hepatic stellate cells. *PLoS One* 9: e101179, 2014.
- Roach KM, Duffy SM, Coward W, Feghali-Bostwick C, Wulff H and Bradding P: The K<sup>+</sup> channel K<sub>Ca</sub>3.1 as a novel target for idiopathic pulmonary fibrosis. *PLoS One* 8: e85244, 2013.
- Roach KM, Feghali-Bostwick C, Wulff H, Amrani Y and Bradding P: Human lung myofibroblast TGF $\beta$ 1-dependent Smad2/3 signalling is Ca(2+)-dependent and regulated by K<sub>Ca</sub>3.1 K(+) channels. *Fibrogenesis Tissue Repair* 8: 5, 2015.
- Sun H, Harris WT, Korytko S, Kotha K, Ostmann AJ, Rezayat A, Sridharan A, Sanders Y, Naren AP and Clancy JP: Tgf-beta down-regulation of distinct chloride channels in cystic fibrosis-affected epithelia. *PLoS One* 9: e106842, 2014.
- Nilius B and Droogmans G: Amazing chloride channels: an overview. *Acta Physiol Scand* 177: 119-147, 2003.
- Zheng YJ, Furukawa T, Tajimi K and Inagaki N: Cl<sup>-</sup> channel blockers inhibit transition of quiescent (G<sub>0</sub>) fibroblasts into the cell cycle. *J Cell Physiol* 194: 376-383, 2003.
- Zheng YJ, Furukawa T, Ogura T, Tajimi K and Inagaki N: M phase-specific expression and phosphorylation-dependent ubiquitination of the ClC-2 channel. *J Biol Chem* 277: 32268-32273, 2002.
- Cheng G, Shao Z, Chaudhari B and Agrawal DK: Involvement of chloride channels in TGF-beta1-induced apoptosis of human bronchial epithelial cells. *Am J Physiol Lung Cell Mol Physiol* 293: L1339-L1347, 2007.
- Zhu L, Yang H, Zuo W, Yang L, Zhang H, Ye W, Mao J, Chen L and Wang L: Differential expression and roles of volume-activated chloride channels in control of growth of normal and cancerous nasopharyngeal epithelial cells. *Biochem Pharmacol* 83: 324-334, 2012.
- Okada Y, Shimizu T, Maeno E, Tanabe S, Wang X and Takahashi N: Volume-sensitive chloride channels involved in apoptotic volume decrease and cell death. *J Membr Biol* 209: 21-29, 2006.
- Mao J, Chen L, Xu B, Wang L, Li H, Guo J, Li W, Nie S, Jacob TJ and Wang L: Suppression of ClC-3 channel expression reduces migration of nasopharyngeal carcinoma cells. *Biochem Pharmacol* 75: 1706-1716, 2008.
- Mao J, Yuan J, Wang L, Zhang H, Jin X, Zhu J, Li H, Xu B and Chen L: Tamoxifen inhibits migration of estrogen receptor-negative hepatocellular carcinoma cells by blocking the swelling-activated chloride current. *J Cell Physiol* 228: 991-1001, 2013.
- Guan YY, Wang GL and Zhou JG: The ClC-3 Cl<sup>-</sup> channel in cell volume regulation, proliferation and apoptosis in vascular smooth muscle cells. *Trends Pharmacol Sci* 27: 290-296, 2006.
- Sang H, Li T, Li H and Liu J: Gab1 regulates proliferation and migration through the PI3K/Akt signaling pathway in intrahepatic cholangiocarcinoma. *Tumour Biol* 36: 8367-8377, 2015.
- Zhou H, Li D, Shi C, Xin T, Yang J, Zhou Y, Hu S, Tian F, Wang J and Chen Y: Effects of exendin-4 on bone marrow mesenchymal stem cell proliferation, migration and apoptosis in vitro. *Sci Rep* 5: 12898, 2015.

27. Zeng R, Xiong Y, Zhu F, Ma Z, Liao W, He Y, He J, Li W, Yang J, Lu Q, *et al*: Fenofibrate attenuated glucose-induced mesangial cells proliferation and extracellular matrix synthesis via PI3K/AKT and ERK1/2. *PLoS One* 8: e76836, 2013.
28. Hitchings RA and Grierson I: Clinico pathological correlation in eyes with failed fistulizing surgery. *Trans Ophthalmol Soc U K* 103: 84-88, 1983.
29. Addicks EM, Quigley HA, Green WR and Robin AL: Histologic characteristics of filtering blebs in glaucomatous eyes. *Arch Ophthalmol* 101: 795-798, 1983.
30. Chen L, Wang L, Zhu L, Nie S, Zhang J, Zhong P, Cai B, Luo H and Jacob TJ: Cell cycle-dependent expression of volume-activated chloride currents in nasopharyngeal carcinoma cells. *Am J Physiol Cell Physiol* 283: C1313-C1323, 2002.
31. Tao R, Lau CP, Tse HF and Li GR: Regulation of cell proliferation by intermediate-conductance  $Ca^{2+}$ -activated potassium and volume-sensitive chloride channels in mouse mesenchymal stem cells. *Am J Physiol Cell Physiol* 295: C1409-C1416, 2008.
32. Chen LX, Zhu LY, Jacob TJ and Wang LW: Roles of volume-activated  $Cl^-$  currents and regulatory volume decrease in the cell cycle and proliferation in nasopharyngeal carcinoma cells. *Cell Prolif* 40: 253-267, 2007.
33. Souktani R, Ghaleh B, Tissier R, d'Anglemont de Tassigny A, Aouam K, Bedossa P, Charlemagne D, Samuel J, Henry P and Berdeaux A: Inhibitors of swelling-activated chloride channels increase infarct size and apoptosis in rabbit myocardium. *Fundam Clin Pharmacol* 17: 555-561, 2003.
34. Small DL, Tauskela J and Xia Z: Role for chloride but not potassium channels in apoptosis in primary rat cortical cultures. *Neurosci Lett* 334: 95-98, 2002.
35. Maeno E, Ishizaki Y, Kanaseki T, Hazama A and Okada Y: Normotonic cell shrinkage because of disordered volume regulation is an early prerequisite to apoptosis. *Proc Natl Acad Sci USA* 97: 9487-9492, 2000.
36. Zhang H, Li H, Yang L, Deng Z, Luo H, Ye D, Bai Z, Zhu L, Ye W, Wang L, *et al*: The  $ClC-3$  chloride channel associated with microtubules is a target of paclitaxel in its induced-apoptosis. *Sci Rep* 3: 2615, 2013.
37. Chen J: The IL-23/IL-17 axis may be important in obesity-associated cancer by way of the activation of multiple signal pathways. *Int J Obes* 34: 1227-1229, 2010.
38. Martelli AM, Evangelisti C, Chiarini F, Grimaldi C, Cappellini A, Ognibene A and McCubrey JA: The emerging role of the phosphatidylinositol 3-kinase/Akt/mammalian target of rapamycin signaling network in normal myelopoiesis and leukemogenesis. *Biochim Biophys Acta* 1803: 991-1002, 2010.
39. Weichhart T and Säemann MD: The PI3K/Akt/mTOR pathway in innate immune cells: emerging therapeutic applications. *Ann Rheum Dis* 67 (Suppl 3): iii70-iii74, 2008.
40. Zhao T, Qi Y, Li Y and Xu K: PI3 kinase regulation of neural regeneration and muscle hypertrophy after spinal cord injury. *Mol Biol Rep* 39: 3541-3547, 2012.
41. Liu P, Cheng H, Roberts TM and Zhao JJ: Targeting the phosphoinositide 3-kinase pathway in cancer. *Nat Rev Drug Discov* 8: 627-644, 2009.
42. Cantley LC: The phosphoinositide 3-kinase pathway. *Science* 296: 1655-1657, 2002.
43. Liu Y, Li W, Liu H, Peng Y, Yang Q, Xiao L, Liu Y and Liu F: Inhibition effect of small interfering RNA of connective tissue growth factor on the expression of extracellular matrix molecules in cultured human renal proximal tubular cells. *Ren Fail* 36: 278-284, 2014.
44. Qin D, Zhang GM, Xu X and Wang LY: The PI3K/Akt signaling pathway mediates the high glucose-induced expression of extracellular matrix molecules in human retinal pigment epithelial cells. *J Diabetes Res* 2015: 920280, 2015.
45. Pan F, Guo R, Cheng W, Chai L, Wang W, Cao C and Li S: High glucose inhibits  $ClC-2$  chloride channels and attenuates cell migration of rat keratinocytes. *Drug Des Devel Ther* 9: 4779-4791, 2015.
46. Heo KS, Ryoo SW, Kim L, Nam M, Baek ST, Lee H, Lee AR, Park SK, Park Y, Myung CS, *et al*:  $Cl^-$  channel is essential for LDL-induced cell proliferation via the activation of Erk1/2 and PI3k/Akt and the upregulation of Egr-1 in human aortic smooth muscle cells. *Mol Cells* 26: 468-473, 2008.
47. Li L, Xia Y, Wang Z, Cao X, Da Z, Guo G, Qian J, Liu X, Fan Y, Sun L, *et al*: Suppression of the PI3K-Akt pathway is involved in the decreased adhesion and migration of bone marrow-derived mesenchymal stem cells from non-obese diabetic mice. *Cell Biol Int* 35: 961-966, 2011.



This work is licensed under a Creative Commons Attribution-NonCommercial-NoDerivatives 4.0 International (CC BY-NC-ND 4.0) License.